DALTON

Effect of ring size in macrocyclic dinuclear manganese(II) complexes upon their structure, properties and reactivity towards H_2O_2 †

Takanori Aono,[a] Hisae Wada,[a] Masami Yonemura,[a] Masaaki Ohba,[a] Hisashi Ōkawa*,[a] and David E. Fenton[b]

[a] *Department of Chemistry, Faculty of Science, Kyushu University, Hakozaki 6-10-2, Higashiku, Fukuoka 812, Japan*
[b] *Department of Chemistry, The University of Sheffield, Sheffield S3 7HF, UK*

A dinuclear manganese(II) complex $[Mn_2L^{4,4}(O_2CMe)_2]$ has been prepared and its structure, properties and catalase-like function studied in comparison with the analogous $[Mn_2L^{m,n}(O_2CMe)_2]$ [m,n = 2,3; 2,4; or 3,3; $(L^{m,n})^{2-}$ denotes macrocycles containing two 2,6-bis(iminomethyl)-4-methylphenolate entities bridged through two lateral chains, $(CH_2)_m$ and $(CH_2)_n$, at the imino nitrogens]. In the centrosymmetric $[Mn_2L^{4,4}(O_2CMe)_2]$ a pair of manganese(II) ions are bridged by two phenolic oxygens of $(L^{4,4})^{2-}$ in the equatorial plane and by two acetate groups at the axial sites. The configuration about each Mn is pseudo-octahedral. The Mn · · · Mn separation is 2.978(1) Å. Cryomagnetic studies (4.2–300 K) indicated a significantly strong antiferromagnetic interaction ($J = -5.0$ cm^{-1} based on $H = -2JS_1S_2$). The complex is oxidized at +0.35 V (*vs*. saturated calomel electrode) at a platinum electrode to a $Mn_2^{II,III}$ complex. It catalyses the disproportionation of hydrogen peroxide in aqueous dimethylformamide. Based on ESR and visible spectroscopic studies, a catalytic mechanism involving the interconversion between $Mn^{II}Mn^{III}$(OH) and $Mn^{II}Mn^{IV}$(=O) species is proposed.

Dinuclear core complexes are of current interest in mimicking bimetallic biosites[1] and in searching for appropriate systems to incorporate and activate simple molecules.[2] The phenol-based macrocycles derived from 2:1:1 condensation of 2,6-diformyl-4-methylphenol, $H_2N(CH_2)_mNH_2$ and $H_2N(CH_2)_nNH_2$, abbreviated as $(L^{m,n})^{2-}$, have been used for the study of homo- and hetero-dinuclear metal complexes.[3–8] One of the advantages in utilizing those macrocycles is that dinuclear cores can be stabilized by the macrocyclic effect[9] and the core structures can be tuned by modification of the macrocycles.[7,8] Dinuclear manganese complexes of the macrocycles have attracted particular attention as being relevant to the mimicking of dimanganese biosites such as manganese catalase (MnCAT),[10] manganese ribonucleotide reductase,[11] *etc*. Previously we reported CAT-like activity of the dinuclear manganese(II) complexes $[Mn_2L^{m,n}(O_2CR)_2]$ (m,n = 2,3; 2,4; or 3,3; R = Me or Ph);[7] in this study an analogous complex $[Mn_2L^{4,4}(O_2CMe)_2]$ has been obtained and structurally characterized. The main emphasis is placed on the ring size effect of $(L^{4,4})^{2-}$ upon the Mn_2 core structure, its properties and reactivity towards hydrogen peroxide.

Experimental

Measurements

Elemental analyses of C, H, and N were obtained at the Elemental Analysis Service Centre of Kyushu University. Analyses of Mn were obtained using a Shimadzu AA-660 atomic absorption/flame emission spectrophotometer. Infrared spectra were recorded on a JASCO IR-810 spectrometer. Molar conductivities were measured at ≈1 × 10^{-3} mol dm^{-3} using a DKK AOL-10 conductivity meter at 20 °C. Electronic spectra were recorded using a Shimadzu MPS-2000 spectrometer, ESR spectra (X-band) on a JEOL JEX-FE3X spectrometer on frozen solutions at liquid-nitrogen temperature. Magnetic susceptibilities were determined on a Faraday balance designed in our laboratory, in the temperature range 80–300 K, and on a HOXAN HSM-D SQUID susceptometer in the range of 4.2–80 K. Calibrations were made using $[Ni(en)_3][S_2O_3]$ (en = ethane-1,2-diamine). Diamagnetic corrections were made using Pascal's constants.[12] Cyclic voltammograms were recorded on an apparatus comprised of a HA-501 potentiostat/galvanostat, HB-104 function generator, and HF-201 coulomb/amperehour meter from Hokuto Denko Ltd. Measurements were carried out using a three-electrode cell equipped with a platinum working electrode, a platinum-coil counter electrode, and a saturated calomel reference electrode (SCE). Tetra-*n*-butylammonium perchlorate was used as the supporting electrolyte. **CAUTION:** it is explosive and should be handled with great care. Coulometry experiments were carried out on the same instrument using a platinum net as the working electrode.

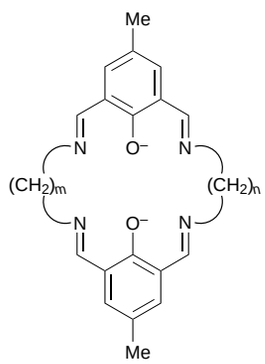

Preparation

2,6-Diformyl-4-methylphenol was prepared by the method of Denton and Suschitzky.[13] All the other chemicals were of reagent grade and used as such.

$[Mn_2L^{4,4}(O_2CMe)_2]$. A mixture of 2,6-diformyl-4-methylphenol (324 mg, 2.0 mmol), 1,4-diaminobutane (264 mg, 3.0 mmol) and manganese(II) acetate tetrahydrate (290 mg, 2.0 mmol) in methanol (50 cm^3) was refluxed for 5 h in an atmosphere of nitrogen. The resulting orange solution was cooled to room temperature and layered with propan-2-ol (20 cm^3). After

† *Non-SI units employed*: $\mu_B \approx 9.27 \times 10^{-24}$ J T^{-1}, G = 10^{-4} T.

3 d yellow microcrystals were formed which were filtered off and dried *in vacuo*. The crude product was dissolved in dichloromethane and the solution was diffused with acetonitrile to form red crystals. Yield 250 mg (38%) (Found: C, 54.8; H, 5.5; N, 8.5. Calc. for $C_{30}H_{36}Mn_2N_4O_6$: C, 54.7; H, 5.5; N, 8.5%). IR(KBr): 2920, 2850, 1830, 1540 and 1400 cm^{-1}. UV/VIS in dimethylformamide (dmf): 380 nm (ε 13300 dm^3 mol^{-1} cm^{-1}). Molar conductance: 8 (in dmf), 21 S cm^{-1} mol^{-1} (in dmf–water, 4:1 v/v).

Catalase-like activity

A closed vessel containing a dmf solution (2 cm^3) of $[Mn_2L^{4,4}(O_2CMe)_2]$ (5 μmol) was stirred at 0 °C on an ice–water bath. Hydrogen peroxide (10.0%, 0.5 cm^3; 1.45 mmol) chilled at 0 °C was injected through a silicon stopper and the dioxygen evolved was measured volumetrically with a burette.

Crystallography

A crystal with approximate dimensions 0.20 × 0.20 × 0.30 mm was sealed in a glass tube and used for X-ray diffraction study. Intensities and lattice parameters were obtained on a Rigaku AFC-7R diffractometer with graphite-monochromated Mo-Kα radiation (λ = 0.710 69 Å) and a 12 kW rotating-anode generator. The data were collected at 20 ± 1 °C using the ω–2θ scan technique to a maximum 2θ value 50.0° at a scan speed of 16.0° min^{-1} (in ω). The weak reflections [$I < 10.0\sigma(I)$] were rescanned (maximum of four scans) and the counts were accumulated to ensure good counting statistics. Stationary background counts were recorded on each side of the reflection. The ratio of the peak counting time to the background counting time was 2:1. The cell parameters were determined from 25 reflections in the range 2θ 29.27–29.23°. The octant measured was $+h$, $+k$, $\pm l$. The intensities of the representative reflections were measured after every 150 reflections. Over the course of data collection the standards increased by 0.2%. An empirical absorption correction based on azimuthal scans of several reflections was applied which resulted in transmission factors ranging from 0.94 to 1.00. A linear correction factor was applied to account for this. Intensity data were corrected for Lorentz-polarization effects. Pertinent crystallographic parameters are summarized in Table 1.

The structure was solved by the direct method and expanded using Fourier techniques. The non-hydrogen atoms were refined anisotropically. Hydrogen atoms were included in the structure-factor calculations but not refined.

Neutral atom scattering factors were taken from Cromer and Waber.[14] Anomalous dispersion effects were included in F_{calc}; the values for $\Delta f'$ and $\Delta f''$ were those of Creagh and McAuley.[15] The values for the mass-attenuation coefficients were those of Creagh and Hubbell.[16] All calculations were performed using the TEXSAN crystallographic software.[17]

Atomic coordinates, thermal parameters, and bond lengths and angles have been deposited at the Cambridge Crystallographic Data Centre (CCDC). See Instructions for Authors, *J. Chem. Soc., Dalton Trans.*, 1997, Issue 1. Any request to the CCDC for this material should quote the full literature citation and the reference number 186/444.

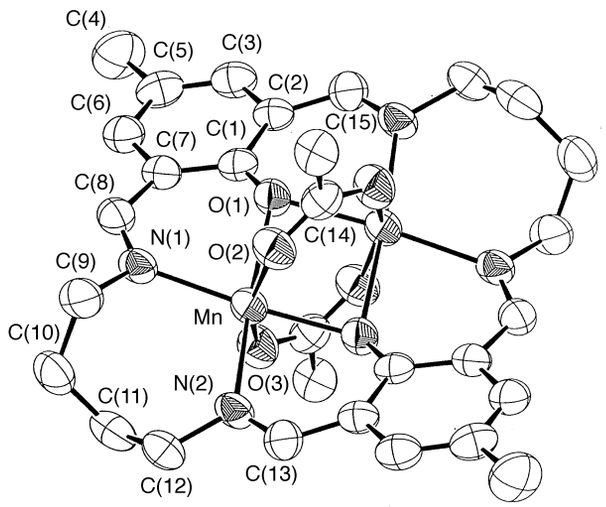

Fig. 1 An ORTEP view of $[Mn_2L^{4,4}(O_2CMe)_2]$

Table 1 Crystallographic data for $[Mn_2L^{4,4}(O_2CMe)_2]$

Formula	$C_{30}H_{36}Mn_2N_4O_6$
Colour	Red
M	658.51
Crystal size/mm	0.20 × 0.20 × 0.30
Crystal system	Monoclinic
Space group	$P2_1/c$ (no. 14)
a/Å	8.847(1)
b/Å	16.425(2)
c/Å	10.152(1)
β/°	98.73(1)
U/Å^3	1458.0(3)
Z	2
D_c/g cm^{-3}	1.500
D_m/g cm^{-3}	1.503
μ(Mo-Kα)/cm^{-1}	9.16
No. reflections with $\|F_o\| \geqslant 3\sigma(\|F_o\|)$	2066
$F(000)$	684
R [a]	0.036
R' [b]	0.030

[a] $R = \Sigma\|\|F_o\| - \|F_c\|\|/\Sigma|F_o|$. [b] $R' = [\Sigma w(\|F_o\| - \|F_c\|)^2/\Sigma w|F_o|^2]^{\frac{1}{2}}$, $w = 1/\sigma(|F_o|)^2$.

Table 2 Selected bond distances (Å) and angles (°) of $[Mn_2L^{4,4}(O_2CMe)_2]$

Mn–O(1)	2.175(2)	Mn–O(1*)	2.144(2)
Mn–O(2)	2.213(2)	Mn–O(3)	2.211(2)
Mn–N(1)	2.180(3)	Mn–N(2)	2.216(3)
Mn · · · Mn*	2.978(1)		
Mn–O(1)–Mn*	87.19(8)	O(1)–Mn–O(1*)	92.81(8)
O(1)–Mn–O(2)	82.08(8)	O(1)–Mn–O(3)	85.68(8)
O(1)–Mn–N(1)	81.50(9)	O(2)–Mn–O(1*)	84.24(8)
O(2)–Mn–N(1)	96.82(9)	O(2)–Mn–N(2)	90.16(9)
O(3)–Mn–O(1*)	81.95(8)	O(3)–Mn–N(1)	95.62(9)
O(3)–Mn–N(2)	101.03(9)	N(1)–Mn–N(2)	102.54(10)
N(2)–Mn–O(1*)	83.36(9)		

Results and Discussion

Crystal structure

The ORTEP[18] view of the complex is shown in Fig. 1 together with the numbering scheme. Selected bond distances and angles are listed in Table 2.

The macrocycle $(L^{4,4})^{2-}$ accommodates two manganese(II) ions within its two N_2O_2 metal-binding sites, providing a centrosymmetric dinuclear core with the nearly coplanar MnO_2Mn skeleton bridged by the phenolic oxygens O(1) and O(1*). The pair of manganese ions are further bridged by two acetate groups above and below the dinuclear skeleton. Thus, the configuration about each Mn is described as a distorted octahedron with O(1), O(1*), N(1) and N(2) of the macrocycle in the equatorial plane and O(2) and O(3) of the acetate groups in the axial sites. The Mn · · · Mn* separation is 2.978(1) Å. The Mn–N and Mn–O bond distances fall in the range 2.144–2.216 Å which is common for manganese(II) complexes.[19,20] The macrocyclic entity, except for the lateral chain part, assumes good coplanarity with an inversion centre at the centre of the dinuclear skeleton formed by Mn, O(1), O(1*) and Mn*. Owing to strain from the deformed $(CH_2)_4$ moiety the N(1)–Mn–N(2) angle

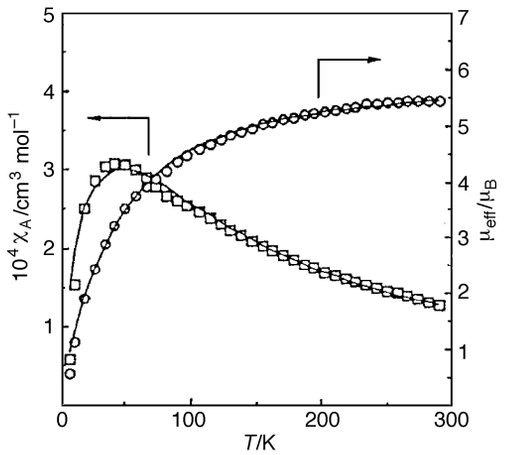

Fig. 2 Temperature dependences of the magnetic susceptibility and magnetic moment (per Mn) of $[Mn_2L^{4,4}(O_2CMe)_2]$. The solid lines are drawn based on the equation given in the text using $J = -5.0$ cm^{-1}, $g = 2.00$ and $\theta = -3.5$ K

[102.5(1)°] is very large compared with the O(1)–Mn–N(1), O(1)–Mn–O(1*) and O(1*)–Mn–N(2) angles [81.50(9), 92.81(8) and 83.36(9)°, respectively].

The core structure of $[Mn_2L^{4,4}(O_2CMe)_2]$ differs from that of previously reported $[Mn_2L^{3,3}(O_2CMe)_2]$.[7] In the latter complex each Mn deviates from the basal N_2O_2 plane by 0.75 Å because of the mismatch between the cavity size and the ionic radius of the manganese(II) ion, and a bidentate acetate group occupies the open space to provide a distorted six-co-ordination about the metal ion. In the case of $[NiMnL^{2,4}(dmf)_2][ClO_4]_2$[8] the Mn^{II} bound at the N_2O_2 site formed by the tetramethylene lateral chain has a distorted six-co-ordinate geometry similar to that of $[Mn_2L^{3,3}(O_2CMe)_2]$. That is, the Mn^{II} is 0.966 Å from the basal N_2O_2 least-squares plane and two dmf molecules occupy the open space. It is likely that Ni^{II} strongly prefers a planar geometry so that the neighbouring N_2O_2 site with the tetramethylene lateral chain has little flexibility to accommodate the larger Mn^{II} within its cavity.

Magnetic properties

The magnetic properties of the complex were studied in the temperature range 4.2–300 K. The temperature dependences of the magnetic susceptibility and magnetic moment (per one Mn) are given in Fig. 2. The magnetic susceptibility increases with decreasing temperature to a maximum value around 45 K and decreases below this temperature. The effective magnetic moment at room temperature is subnormal (5.44 μ_B) and decreases with decreasing temperature to 0.57 μ_B at 7.1 K. The results strongly suggest an antiferromagnetic interaction operating between the manganese(II) ions. Magnetic simulations have been made on the basis of the isotropic Heisenberg model $H = -2JS_1S_2$ including the Weiss term θ to correct for secondary effects. The magnetic susceptibility expression (1) is applicable for the case of $S_1 = S_2 = \frac{5}{2}$. Here N is Avogadro's number, β the Bohr magneton, k the Boltzmann constant, T the absolute temperature, g the Zeeman splitting factor and J the exchange integral. As indicated by the solid line in Fig. 2, the cryomagnetic property of the complex can be well reproduced by

$$\chi_A = Ng^2\beta^2/k(T - \theta)A/B \quad (1)$$

$$A = \exp(-28J/kT) + 5\exp(-24J/kT) + 14\exp(-18J/kT) + 30\exp(-10J/kT) + 55 \quad (2)$$

$$B = \exp(-30J/kT) + 3\exp(-28J/kT) + 5\exp(-24J/kT) + 7\exp(-18J/kT) + 9\exp(-10J/kT) + 11 \quad (3)$$

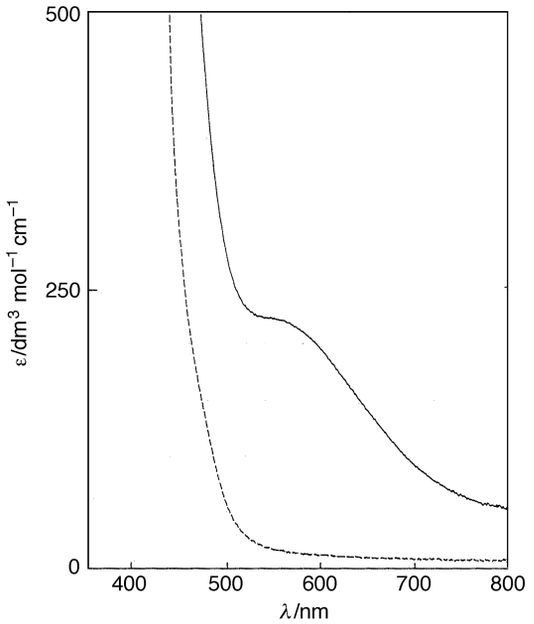

Fig. 3 Visible spectrum of the mixed-valence $Mn_2^{II,III}$ complex prepared by coulometry of $[Mn_2L^{4,4}(O_2CMe)_2]$ at +0.33 V. The dotted line indicates the spectrum of $[Mn_2L^{4,4}(O_2CMe)_2]$

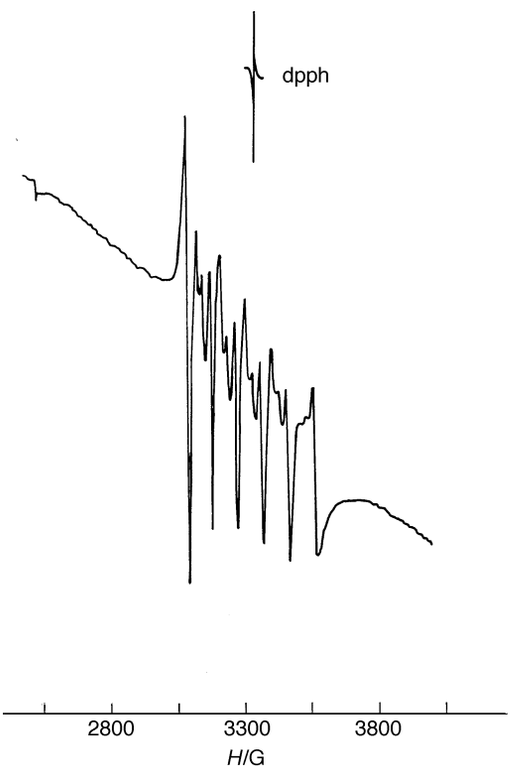

Fig. 4 The ESR spectrum of the mixed-valence $Mn_2^{II,III}$ complex. dpph = Diphenylpicrylhydrazyl

expression (1) using $J = -5.0$ cm^{-1}, $g = 2.00$ and $\theta = -3.5$ K. The discrepancy factor defined as $R(\chi) = [\Sigma(\chi_{obs} - \chi_{calc})^2/\Sigma(\chi_{calc})^2]^{\frac{1}{2}}$ is 7.6×10^{-2}.

The magnetic interaction observed is strongly antiferromagnetic whereas that in $[Mn_2L^{3,3}(O_2CMe)_2]$ is very weak and ferromagnetic ($J = +0.4$ cm^{-1}).[7] It is important to determine the magnetostructural correlation for the two complexes. In $[Mn_2L^{4,4}(O_2CMe)_2]$ the two basal N_2O_2 planes are nearly coplanar and two manganese ions reside on the coplane. In $[Mn_2L^{3,3}(O_2CMe)_2]$ the basal N_2O_2 planes are also coplanar but the two manganese(II) ions are 0.75 Å from the coplane in opposite directions. Thus, the least-squares plane of the

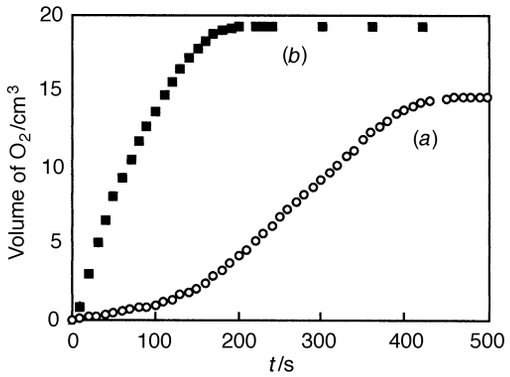

Fig. 5 Time course of oxygen evolution in the decomposition of H_2O_2 by $[Mn_2L^{4,4}(O_2CMe)_2]$ (*a*) and $[Mn_2L^{3,3}(O_2CMe)_2]$ (*b*)

MnO_2Mn skeleton is tilted by 19.47° from the basal $N_2O_2N_2$ coplane. It is known that phenolic oxygen bridges can contribute to magnetic superexchange in di-μ-phenoxo-dimetal complexes mainly through its 2p orbitals.[21] In the case of $[Mn_2L^{4,4}(O_2CMe)_2]$ the $2p_x$ and $2p_y$ orbitals of the phenolic oxygens have their lobes spread on the coplane, allowing an efficient overlapping between manganese 3d orbital and phenolic 2p orbital. The overall exchange integral J for dinuclear manganese(II) is given by the mean of 25 (= 5 × 5) individual exchange integrals $j(a,b)$ between the ath unpaired electron of Mn^1 and bth unpaired electron of Mn^2, *i.e.* $J = \Sigma j(a,b)/25$.[22] In the present complex the main contribution to the negative exchange integral ($J = -5.0$ cm^{-1}) may be $j(d_{x^2-y^2},d_{x^2-y^2})$ as demonstrated for strongly antiferromagnetic di-μ-phenoxo-dicopper(II) complexes.[23,24] Such an efficient overlapping between the manganese 3d orbital and phenolic 2p orbital is not expected for $[Mn_2L^{3,3}(O_2CMe)_2]$ because of the large deviation of the two manganese ions from the basal $N_2O_2N_2$ coplane.

Mixed-valence $Mn_2^{II,III}$ complex

The electrochemical properties of the complex have been studied by cyclic voltammetry in dmf (platinum electrode). This shows one pseudo-reversible couple near +0.35 V vs. SCE which is assigned to the $Mn^{II}Mn^{II}$–$Mn^{II}Mn^{III}$ process based on coulometry studies at +0.33 V. The electrolysed solution is brown and shows an absorption band at 560 nm (ε 240 dm^3 mol^{-1} cm^{-1}) which can be assigned to a d–d component of Mn^{III} ion (see Fig. 3). Except for this band no prominent absorption is seen in the near-infrared region, suggesting a spin-trapped electronic state (Class I) of the mixed-valence complex. The ESR spectrum of the electrolysed solution (frozen at liquid-nitrogen temperature) shows a six-line hyperfine structure and a weaker 10-line hyperfine structure (Fig. 4). Such an ESR spectral feature is characteristic of a mixed-valence $Mn_2^{II,III}$ complex comprised of essentially uncoupled manganese-(II) and -(III) ions.[7,20] The strong six-line hyperfine structure is assigned to the $\Delta M_I = 0$ spin-allowed transitions and the weaker 10-line structure to the $\Delta M_I = 1$ spin-forbidden transitions of Mn^{II}. A similar ESR spectrum of a $Mn_2^{II,III}$ complex has been obtained from dinuclear manganese(II) complexes of $(L^{2,3})^{2-}$, $(L^{2,4})^{2-}$ and $(L^{3,3})^{2-}$.[7]

CAT-like activity

The CAT-like activity of the complex to disproportionate H_2O_2 into H_2O and O_2 was examined in dmf at 0 °C by volumetric measurements of evolved dioxygen. The time course of the oxygen evolution at a complex concentration of 2.5×10^{-3} mol dm^{-3} is shown in Fig. 5. For comparison the time course of the catalysis by $[Mn_2L^{3,3}(O_2CMe)_2]$ under the same conditions is also given. In the catalysis by the present complex the initial rate was very low but after a lag time (*ca.* 150 s) the rate significantly increased. In the catalysis by $[Mn_2L^{3,3}(O_2CMe)_2]$ the oxygen evolution was observed without a lag time. Thus, the CAT-like activity of $[Mn_2L^{4,4}(O_2CMe)_2]$ is low relative to that of $[Mn_2L^{3,3}(O_2CMe)_2]$. It has been shown that the bidentate acetate group of $[Mn_2L^{3,3}(O_2CMe)_2]$ is substitution labile in aqueous dmf and this site is available for the accommodation of hydrogen peroxide in the catalase-like reaction. In this study we have noticed that $[Mn_2L^{4,4}(O_2CMe)_2]$ shows a small electric conductivity in aqueous dmf (dmf–water, 4:1 v/v) corresponding to the CAT-like activity study. This fact indicates considerable inertness of the bridging acetate group and explains the low catalytic activity of $[Mn_2L^{4,4}(O_2CMe)_2]$ at the initial stage of the H_2O_2 decomposition reaction. Dissociation of the bridging acetate group, however, may occur with time as indicated by the gradual increase in the O_2-evolution rate.

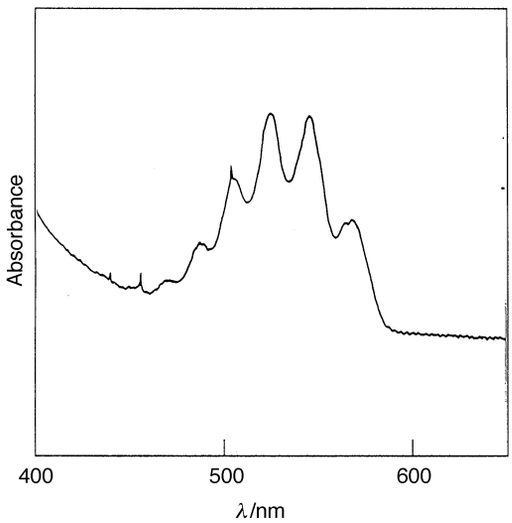

Fig. 6 The characteristic c.t. band observed upon decomposition of H_2O_2 by $[Mn_2L^{4,4}(O_2CMe)_2]$ (1.0×10^{-3} mol dm^{-3}) at 0 °C

In the previous study[7] using dinuclear maganese complexes of $(L^{2,3})^{2-}$, $(L^{2,4})^{2-}$ and $(L^{3,3})^{2-}$, it was shown that the CAT-like function proceeds by an intermolecular mechanism through the interconversion between $Mn^{II}Mn^{III}$ [probably $Mn^{II}Mn^{III}(OH)$] and $Mn^{II}Mn^{IV}(=O)$ species. The involvement of the latter species is evidenced by the characteristic oxo-to-manganese(IV) charge-transfer (c.t.) band near 530 nm bearing ν(Mn=O) vibration modes of *ca.* 730 cm^{-1}.[25,26] The c.t. band can be detectable only when the $Mn^{II}Mn^{IV}(=O)$ species has a long lifetime relative to the time-scale of visible spectroscopy.[7] This can be realized when the catalytic cycle between $Mn^{II}Mn^{III}(OH)$ and Mn^{II}-$Mn^{IV}(=O)$ is slowed by lowering the reaction temperature or the complex concentration. In the present case, the characteristic c.t. band could be observed when the reaction was carried out at 0 °C and at the complex concentration of 1×10^{-3} mol dm^{-3} (see Fig. 6). The result clearly demonstrates that the Mn^{II}-$Mn^{IV}(=O)$ species is involved in the catalytic process.

The reaction mixture was subjected to ESR spectroscopic studies at liquid-nitrogen temperature. The spectrum was exactly the same as that of the mixed-valence $Mn_2^{II,III}$ complex prepared by coulometry (Fig. 4). We may conclude that $[Mn_2L^{4,4}(O_2CMe)_2]$ catalyses the disproportionation of H_2O_2 by the interconversion between $Mn_2^{II,III}$ and $Mn_2^{II,IV}$, the same mechanism as proposed for $[Mn_2L^{3,3}(O_2CMe)_2]$.[7]

From the O_2-evolution profile (Fig. 5) the yield of dioxygen is about 75% of the theoretical amount for catalysis by $[Mn_2L^{4,4}(O_2CMe)_2]$ compared with 100% for the catalysis by $[Mn_2L^{3,3}(O_2CMe)_2]$. Such a decrease in the yield of dioxygen has been found when a pair of manganese ions are not equivalent in electronic nature.[26] The interaction of H_2O_2 with two non-equivalent manganese centres may lead, more or less, to a heterolytic fission of the O–O bond of hydrogen peroxide. However, this is not the case for $[Mn_2L^{4,4}(O_2CMe)_2]$ which has

two equivalent manganese ions. We presume that the N_2O_2 cavity of $(L^{4,4})^{2-}$ is too large to accommodate the small Mn^{IV} and so the Mn^{IV} formed in the CAT-like catalysis oxidizes the ligand of the complex.

The present study adds a support to the proposal that the MnCAT-like activity of the dinuclear manganese complexes of $(L^{m,n})^{2-}$ proceeds by an intermolecular mechanism through the interconversion of $Mn_2^{II,III}$ and $Mn_2^{II,IV}$ species.

Acknowledgements

This work was supported by a Grant-in-Aid for Scientific Research (No. 07454178) from the Ministry of Education, Science and Culture, Japan. Thanks are also due to The Daiwa Anglo-Japanese Foundation and The British Council for support of the collaborative research project.

References

1 D. E. Fenton and H. Ōkawa, *Perspectives on Bioinorganic Chemistry*, eds. R. W. Hay, J. R. Dilworth and K. B. Nolan, JAI Press, London, 1993, vol. 2, pp. 81–138.
2 P. A. Vigato, S. Tamburini and D. E. Fenton, *Coord. Chem. Rev.*, 1990, **106**, 25.
3 H. Ōkawa and S. Kida, *Inorg. Nucl. Chem.*, 1971, **7**, 751; *Bull. Chem. Soc. Jpn.*, 1972, **45**, 1759; M. Tadokoro, H. Ōkawa, N. Matsumoto, M. Koikawa and S. Kida, *J. Chem. Soc., Dalton Trans.*, 1991, 1657; M. Tadokoro, H. Sakiyama, N. Matsumoto, M. Kodera, H. Ōkawa and S. Kida, *J. Chem. Soc., Dalton Trans.*, 1992, 313; H. Ōkawa, J. Nishio, M. Ohba, M. Tadokoro, N. Matsumoto, M. Koikawa, S. Kida and D. E. Fenton, *Inorg. Chem.*, 1993, **32**, 2949.
4 N. H. Pilkington and R. Robson, *Aust. J. Chem.*, 1970, **23**, 2225; B. F. Hoskins, R. Robson and G. A. Williams, *Aust. J. Chem.*, 1975, **28**, 2598; *Inorg. Chim. Acta*, 1975, **29**, 2607; 1976, **16**, 16, 121.
5 R. R. Gagne, C. A. Koval and T. J. Smith, *J. Am. Chem. Soc.*, 1977, **99**, 8367; R. R. Gagne, C. A. Koval, T. J. Smith and M. C. Cimolino, *J. Am. Chem. Soc.*, 1979, **101**, 4571; R. R. Gagne, C. L. Spiro, T. J. Smith, C. A. Hamann, W. R. Thies and A. K. Shiemke, *J. Am. Chem. Soc.*, 1981, **103**, 4073; C. L. Spiro, S. L. Lambert, T. J. Smith, E. N. Duesler, R. R. Gagne and D. N. Hendrickson, *Inorg. Chem.*, 1981, **20**, 1229; S. L. Lambert, C. L. Spiro, R. R. Gagne and D. N. Hendrickson, *Inorg. Chem.*, 1982, **21**, 68; R. C. Longe and D. N. Hendrickson, *J. Am. Chem. Soc.*, 1982, **105**, 1513.
6 S. K. Mandal and K. Nag, *J. Chem. Soc., Dalton Trans.*, 1983, 2429; 1984, 2141; S. K. Mandal, B. Adhikary and K. Nag, *J. Chem. Soc., Dalton Trans.*, 1986, 1175.
7 H. Wada, K. Motoda, M. Ohba, H. Sakiyama, N. Matsumoto and H. Ōkawa, *Bull. Chem. Soc. Jpn.*, 1995, **68**, 1105.
8 H. Wada, T. Aono, K. Motoda, M. Ohba, N. Matsumoto and H. Ōkawa, *Inorg. Chim. Acta*, 1996, **246**, 13.
9 J. D. Lamb, R. M. Izatt, J. J. Christensen and D. J. Eatough, *Coordination Chemistry of Macrocyclic Compounds*, ed. G. A. Melson, Plenum, New York, 1979, p. 145.
10 R. M. Fronko, J. E. Penner-Hahn and C. J. Bender, *J. Am. Chem. Soc.*, 1988, **110**, 7554; G. S. Allgood and J. J. Perry, *J. Bacteriol.*, 1986, **168**, 563.
11 A. Willing, H. Follmann and G. Auling, *Eur. J. Biochem.*, 1988, **170**, 603.
12 E. A. Boudreaux and L. N. Mulay, *Theory and Applications of Molecular Paramagnetism*, Wiley, New York 1976, pp. 491–494.
13 D. A. Denton and H. Suschitzky, *J. Chem. Soc.*, 1963, 4741.
14 D. T. Cromer and J. T. Waber, *International Tables for X-Ray Crystallography*, Kynoch Press, Birmingham, 1974, vol. 4.
15 D. C. Creagh and W. J. McAuley, *International Tables for X-Ray Crystallography*, ed. A. J. C. Wilson, Kluwer, Boston, 1992, pp. 219–222.
16 D. C. Creagh and H. H. Hubbell, *International Tables for X-Ray Crystallography*, ed. A. J. C. Wilson, Kluwer, Boston, 1992, pp. 200–206.
17 TEXSAN, Molecular Structure Corporation, Houston, TX, 1985.
18 C. K. Johnson, ORTEP, Report 3794, Oak Ridge National Laboratory, Oak Ridge, TN, 1965.
19 D. Luneau, J.-M. Savarriault, P. Cassoux and J.-P. Tuchagues, *J. Chem. Soc., Dalton Trans.*, 1988, 1225.
20 H.-R. Chang, S. K. Larsen, P. D. W. Boyd, C. G. Pierpont and D. N. Hendrickson, *J. Am. Chem. Soc.*, 1988, **110**, 4565.
21 P. J. Hay, J. C. Thibault and R. Hoffmann, *J. Am. Chem. Soc.*, 1975, **97**, 4884.
22 O. Kahn, *Molecular Magnetism*, VCH, Weinheim, 1993.
23 M. Melnik, *Coord. Chem. Rev.*, 1982, **42**, 259.
24 C. J. Cairns and D. H. Busch, *Coord. Chem. Rev.*, 1986, **69**, 1.
25 H. Sakiyama, H. Ōkawa and R. Isobe, *J. Chem. Soc., Chem. Commun.*, 1993, 882; H. Sakiyama, H. Ōkawa and M. Suzuki, *J. Chem. Soc., Dalton Trans.*, 1993, 3823.
26 C. Higuchi, H. Sakiyama, H. Ōkawa, R. Isobe and D. E. Fenton, *J. Chem. Soc., Dalton Trans.*, 1994, 1097.

Received 11*th November* 1996; *Paper* 6/07658K